Powder Technology 360 (2020) 120–128

Contents lists available at ScienceDirect

Powder Technology

journal homepage: www.elsevier.com/locate/powtec

Numerical study on the influence of fine particle deposition characteristics on wall roughness

Wenpeng Hong, Bihui Wang, Jianxiang Zheng *

School of Energy and Power Engineering, Northeast Electric Power University, Jilin, 132012, China

ARTICLE INFO

Article history:
Received 21 March 2019
Received in revised form 13 August 2019
Accepted 30 September 2019
Available online 12 October 2019

Keywords:
Gas-solid two phase flow
CFD-DEM
Particle deposition
Rib-roughened surface

ABSTRACT

This paper presents a study of the characteristics of a 1–50 μm particle deposition in a rib-roughened channel using a combined computational fluid dynamics-discrete element method (CFD-DEM). The effects of particle size, roughness element shape and surface energy on the deposition ratio are defined. Notably, The deposition rate of small particles ($0.1<\tau_p^+<1$) is greatly improved, the particle size of medium particle size ($1<\tau_p^+<10$) is small, However, the large particles ($\tau_p^+>10$) have a lower deposition rate due to larger mass and inertia; Due to the different angles between the windward and leeward surfaces of rough elements with different shapes and the direction of airflow, the velocity fluctuation of the flow field in the duct and the eddies near the rough elements can make obvious changes. The deposition rate of a sharp-angle rough structure was the highest, while that of a triangular rough structure was the lowest. And the increase of surface energy the particles deposition rate increase.

1. Introduction

Particulate matter is ubiquitous in nature and in engineering applications. Smoke, dust, fog, haze and other fine particles are often suspended in the air to pollute the environment. The International Organization for Standardization GB/T15604-2008 specifies that solid suspensions with a particle size of less than 75 μm are defined as dust. Dust particles ($d_p < 75$ μm) in urban environment the main pollution factors [1]. Several modern-day activities produce these fine particles, including pulverized coal combustion in power plants, automobile exhaust gas and building flue gas emissions. Their combined emission make the dust particles in the atmosphere increase sharply, causing serious harm to urban air quality and affecting human health [2]. When airflow carries particles through a wall, particles will collide with the wall, roll, slide and jump up and down due to the gravity of particles and the interaction between airflow and particle, but they eventually deposit on the wall. The fine particles are more likely to deposit on the wall because of their greater adhesion tendencies. It is found that the arrangement of rib elements in a channel can help improve the performance of a particle removal device [3,4]. The main reason is that a rough structure not only affects the air flow near the wall, but also has a strong interception effect on the incoming particles. However, rough structures of different shapes have different effects on airflow and particle interception. Therefore, it is of great significance to study the effect of rough elements with different shapes on the wall deposition of particles in the channel for cleaning and particle removal.

Due to environmental and industrial production needs, a comprehensive understanding of particle deposition is becoming increasingly important. At present, most scholars use experimental and numerical simulation methods to study the deposition of particulate matter in channels. Papavergos and Hedley [5] as well as Reeks [6], and Wood [7] proposed an empirical formula for three subsidence zones (diffusion zone, diffusion collision zone and inertial buffer zone) in the horizontal channel turbulent flow. Sippola [8] compares the above empirical formulas with Liu & Agarwal's [9] experimental data, which shows the Wood empirical formula to be more in line with the experimental results. Sommerfeld et al. [10] carried out an experimental analysis of a gas particle flow in narrow channels from two aspects of particle velocity distribution and pressure loss. They found that the roughness makes the particle distribution in the channel more uniform. The effect of wall roughness on particle concentration distribution decreases with the increase of particle size. Deshmukh [11] used high-speed particle tracking velocimetry and found that small particles are easier to disperse in channels than large particles. With the increase of mass load ratio, particles are easier to accumulate at the bottom of the pipeline. Barth et al. [12] recorded the turbulent flow field between periodic ribs using a three-dimensional particle image velocimetry (PIV) system. The structure of intercostal granular deposits was measured by a laser distance sensor. The accumulation of granular layers varies linearly with time. Particle

* Corresponding author.
E-mail address: 59748529@qq.com (J. Zheng).

https://doi.org/10.1016/j.powtec.2019.09.079
0032-5910/

impact, turbulent dispersion and gravity settlement have some effects on the thickness distribution of multi-layer deposits. Subsequently, Lecrivain et al. [13,14] studied the multilayer deposition process of aerosol particles in turbulent channels by numerical simulation. Zhao et al. [15] proposed an improved Eulerian model, which was used to predict the rate of particle deposition on the rough wall in a fully developed turbulent flow. They found that the dimensionless deposition velocity increases with the roughness. Milici [16] considered the elastic rebound of particles on a rough wave wall. The influence of particles on a turbulent flow field was analyzed. The results show that the particles near the wall surface flow to the flow area at a higher velocity. Matsusaka et al. [17] found that the deposition and re-entrainment of turbulent aerosol particles can form granular deposits layers. Among them, micron-sized particles tend to form zonal and film-like deposits. Submicron particles only form a film-like deposit layer. The thickness of the sedimentary layer is analyzed theoretically. Lo Iacono et al. [18] used large eddy simulation (LES) and Lagrange particle tracking techniques. The dynamic behavior differences of spherical and cylindrical particles in single-surface ribbed channel flow were studied. The results show that spherical particles mainly concentrate on the front surface of ribs, while cylindrical particles are not as likely to stick. At present, there are few studies on coarse wall particle deposition, and most scholars use clear large-scale obstacles to approximately replace the surface roughness. Lai et al. [19,20] used neutron activation to label particles. The aerosol particle deposition in fully developed turbulent flow fields with duplicate ribs on the surface was experimentally investigated. The spatial distribution of aerosol particles on a rib surface was monitored. It was found that repeated ribs on the surface resulted in an increase in pressure. In addition, particle resuspension and rebound reduce particle deposition on rib surface. Recently, H Lu and L Lu [21,22] combined their discrete particle model (DPM) with a Reynolds stress model (RSM), using a numerical simulation method. The particle deposition in a two-dimensional rectangular pipe with a rough structure was simulated numerically. At the same time, the effects of height-span ratio between a rough structure and the layout of a rough structure on particle deposition were studied. The height-span ratio study shows that the particle deposition on a rough wall is higher than that on a smooth wall. Dritselis et al. [23] found that the increase of a particle deposition coefficient on the rough surface is closely related to the mechanism of direct inertial collision and interception. The number of particles deposited on the back surface of the square column was very small. This shows that an increase in the effective deposition area does not necessarily mean an increase particle removal. In recent years, the discrete element method (DEM) has been widely used in the study of gas-solid two-phase flow. The process of particle deposition belongs to the process of adhesive contact between particles. The adhesion between particles and walls is mainly due to the force between particles or between particles and walls. Adsorption between particles and adherent substrates is achieved by force. Afkhami et al. [24] uses large eddy simulation and the discrete element method. The turbulent particle flows such as particle diffusion and agglomeration in the channel were studied, and results showed that the surface energy of particles is positively correlated with the agglomeration rate. Zhang [25] describes a particle trajectory and collision process by the discrete element method. They found that the collision between particles in the near wall region enhances the diffusion of particles along a vertical direction. At the same time, the resuspension rate of particles near the channel or chute bottom has a great influence. Li Shuiqing et al. [26] used the Johnson, Kendall and Roberts (JKR) model to simulate the deposition and aggregation of particles in gas-solid dilute phase flow. The deposition process of particles on fibers was analyzed. The results show that micron-sized particles are easier to deposit near the central streamline of the pipeline.

However, the effect of adhesion force on particle deposition was rarely considered in previous studies. In the contact process between particles and the wall surface, particles are deposited or detached from the wall due to van der Waals adhesion force and the interaction between airflow and particles. Notably, the van der Waals adhesion force is larger than the force of gravity with a decrease in particle size through the analysis of force on particles with a diameter of 1–50 μm, which makes it necessary to analyze the influence of adhesion force on particle deposition. At the same time, in previous studies, it was generally considered that the particles were considered to be deposited after contact with the wall surface. Therefore, the rebound effect between particles, particles and walls was considered.

Therefore, it is necessary to conduct in-depth research on particle deposition. It not only reveals the inherent laws of natural phenomena (such as the deposition of dust particles in the respiratory system)and industrial applications (such as ash deposition on the surface of heat exchangers and photovoltaic modules). At the same time, it is of great significance to the motion of micron particles under the action of multi-field. In this paper, the discrete element method (DEM) is coupled with computational fluid dynamics (CFD). Based on the JKR contact theory of the van der Waals adhesion force, the deposition of micron-sized particles on a rough surface was studied. The purpose of this paper is to discuss the effect of different rough structures on particle deposition and obtain the distribution of particles on rough walls.

2. Physical model and computational cases

In this paper, a three-dimensional (3D) rectangular rough flow channel was selected as the research object, and the rough structures with different shapes (square, sharp corner, triangle) are arranged. The total length of flow channel X is 460 mm, and the cross section of square D is 20 mm and is shown in Fig. 1. To ensure the full development of the air, the first half of the channel is smooth, and the second half is arranged with nine rough elements on the upper and lower walls respectively. Rough element spacing for P is 20 mm, and height e is 2 mm. Thirty-two different calculation cases were studied and the detailed parameters of each case are shown in Tables 1-3.

3. Numerical method and validation

3.1. Numerical model

The gas phase is composed of constant physical properties and an incompressible fluid. The governing equations include the continuity equation and momentum equation. Because the gas-solid two-phase flow is mostly turbulent in practical engineering, an accurate turbulence model has a great influence on the treatment of particle movement. Some scholars only use the k-e model to simulate grain deposition, but the resulting deposition rates are too high. This is mainly due to the isotropic assumption of turbulent fluctuation in a k-e model which obtains a turbulent fluctuation velocity near the wall that is too high resulting in an exaggerated deposition. Therefore, the Reynolds stress model (RSM), which takes into account the anisotropy of turbulence, can accurately simulate complex near-wall flows [27].

The particle phase is determined by DEM method. The JKR model is used to solve the collision contact forces between particles and between particles and walls. At the same time, the friction between particles and the wall, such as rolling friction and sliding friction is considered. The ratio of particle volume to air volume is 0.0186% in the whole calculation domain, which is much less than 5%,

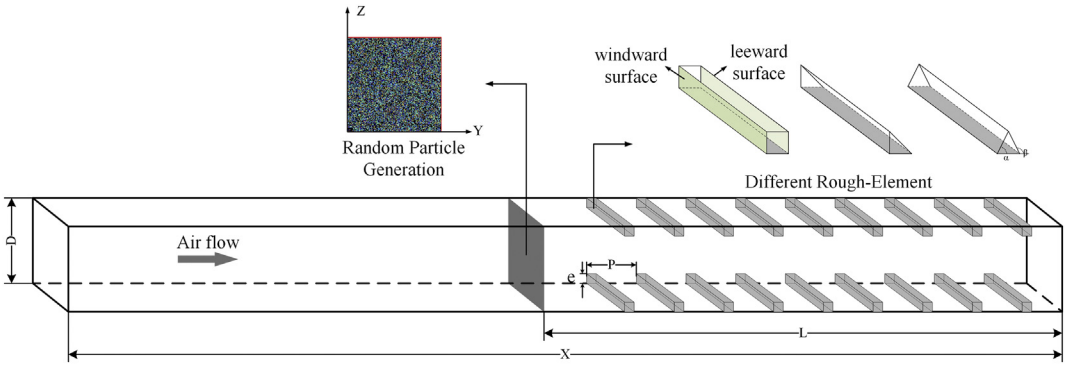

Fig. 1. Schematic of rough channel with rough-element.

Table 1
Calculating conditions.

Case no.	Air velocity (m/s)	Particle diameter (μm)	Surface type	Surface energy (J/m^2)
A (1–8)	5	1, 2, 3, 5, 10, 20, 30, 50	Smooth	0.01
B (9–16)	5	1, 2, 3, 5, 10, 20, 30, 50	Square Rough Element	0.01
C (17–24)	5	1, 2, 3, 5, 10, 20, 30, 50	Sharp-angle Rough Element	0.01
D (25–32)	5	1, 2, 3, 5, 10, 20, 30, 50	Triangular Rough Element	0.01
E (33–43)	5	10,50	Triangular Rough Element	0.01,0.03,0.05,0.07,0.1

therefore the influence of particles on gas can be neglected [28,29]. The particle motion equation follows:

$$m_p \frac{du_{pi}}{dt} = F_D + m_p g + F_{L,saffman} + F_{po} + F_{contact} + F_{Mag} \quad (1)$$

$$I\frac{d\vec{\Omega}}{dt} = M_F + M_A \quad (2)$$

where u_{pi} is the particle translation velocity, m_p is the particle mass, I is the particle rotation inertia, Ω is the particle rotation velocity. The particle drag force, the particle gravity, Saffman lift force, van der Waals adhesion force and Contact force and Magnus force are given on the right side of Eq. (1). The fluid action moment, the van der Waals adhesion moment and the particle collision moment are expressed on the right side of Eq. (2).

3.2. Boundary conditions and solution methods

In the simulation of gas flow, the velocity inlet is used on the left side, the outflow is used on the right side, and the no-slip boundary condition is used on the wall. To fully develop air turbulence in a tube, 20,000 particles are released at X = 260 mm. The gas phase and particle phase parameters are shown in Table 2.

The SIMPLE algorithm is used for the coupling of gas pressure and velocity. The convection term is discretized by the second-order upwind scheme, and the diffusion term is discretized by the central difference scheme. The particle phase is calculated by the discrete element method (DEM), and the viscous force model is based on the JKR model. Ansys-Fluent software was used to simulate the gas phase and discrete element. Rocky software was used to simulate the particle phase.

Table 2
Particle parameter setting.

Parameters	Value
Particle density kg·s/m	2450
Gas dynamic viscosity kg·s/m	1.7894×10^{-5}
Gas density kg/m^3	1.225
Poisson ratio	0.3
Temperature K	288

3.3. Particle deposition process

Particles usually collide, roll, slide and adhere to the wall when they pass through by the wall with incoming gas flow. Assuming that the particles are immersed in the viscous bottom, the hydrodynamic forces are mainly caused by viscous shear flow, including air drag force (F_D)

Table 3
Verification of vortex length near rough elements.

	P1/e	P2/e	P3/e	P4/e
RSM	0.95	0.91	0.6	4.1
DES [12]	1.06	0.81	0.88	4.12
Experiment [30]	1–1.5	0.6–0.9	0.2–0.3	3.7–3.9

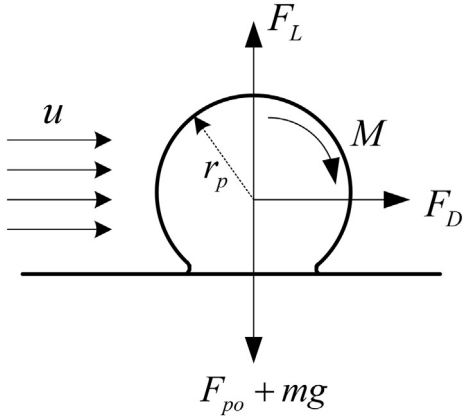

Fig. 2. Forces and moments of particles deposited on the wall.

and shear lift force (F_L). Fig. 2 shows the force acting on the wall after the particles contact. In the simple force balance model, the reason why particles leave the wall in the air flow field is that the normal component of the fluid force is equal to the separation force. The air velocity near the wall can be expressed by the mean value and fluctuating component. The fluid forces acting on the particles are also calculated by summing up the mean value (shear layer) and the fluctuating component (viscous structure layer).

For the convenience of comparison, the forces are converted into dimensionless form, that is, F is expressed as F^+:

$$F^+ = \frac{F}{\nu^2\rho} \tag{3}$$

Dimensionless distance and dimensionless radius are introduced as:

$$y^+ = \frac{yu^*}{\nu} \tag{4}$$

$$r_p^+ = \frac{r_p u^*}{\nu} \tag{5}$$

where y^+ is the dimensionless distance from the wall, y is the distance from the wall, and ν is the kinematic viscosity of air. u^* is the frictional velocity, which can be calculated by:

$$u^* = \sqrt{\tau_w/\rho} \tag{6}$$

O'Neill [30] proposed an analytical solution of linearized N–S equation for spherical particles in viscous fluid given as:

$$F_D = 6\pi\mu\frac{du}{dy}r_p^2\psi \tag{7}$$

where Ψ, the Stokes drag force correction factor, considering wall effect is 1.7009. Thus, the dimensionless drag force is obtained by:

$$F_D^+ = 32.04\left(r_p^+\right)^2 \tag{8}$$

Saffman proposed an average lifting force for small particles in low-speed shear flow as:

$$F_{L,saffman} = 1.62\mu d_p^2\frac{du/dy}{\sqrt{\nu|du/dy|}}(u-u_{px}) \tag{9}$$

The average lifting force in viscous shear layer is defined by:

$$F_{L,saffman}^+ = 6.48\left(r_p^+\right)^3 \tag{10}$$

The dimensionless lifting force of a pulsating shear layer is defined by:

$$F_{L1}^+ = 0.88\left(r_p^+\right)^4 \tag{11}$$

The lifting force perpendicular to the mainstream is defined by:

$$F_{L2}^+ = 0.16\left(r_p^+\right)^3 \tag{12}$$

In the JKR model, a force proposed to pull particles off the wall is defined by:

$$F_{po} = \frac{3}{2}\pi\gamma r_p \tag{13}$$

where γ is solid surface energy. The friction coefficient between the wall and the particles is μ_f, considering the sliding condition of the particles on the wall,

$$F_D^+ \geq \mu_f\left(F_{po}^+ + G^+ - F_L^+\right) \tag{14}$$

The rolling conditions of particles on the wall can be expressed as:

$$F_D^+ \geq 0.57\frac{r_{eq}}{r_p}\left(F_{po}^+ + G^+ - F_L^+\right) \tag{15}$$

where r_{eq} is the contact radius between the particle and the wall surface when the particle deforms. The deposition conditions of particles on the wall can be expressed as:

$$F_L^+ > F_a^+ \tag{16}$$

The variation trend of forces with dimensionless radius are shown in Fig. 3 where $\tau_p^+ < 1$. Because the lifting force is small relative to the surface force, it is difficult for the particles to be pulled away from the wall by the airflow after the particles are deposited on the wall. At this time, the rolling and sliding of particles are easier to achieve.

3.4. Mesh and model validation

3.4.1. Grid resolution

Using structured grid to partition computing areas. In order to accurately predict the near-wall flow characteristics, The upper and lower walls of rough channel are meshed. The height of the first layer is 0.05 mm, the growth factor of 1.2. The grid independence verification of the square rough element channel is carried out. The average wind speed on the windward side of the sixth to ninth rough elements is taken as the detection parameter. As shown in Fig. 4 the simulation results are basically the same when the number of grids is greater than 1,776,245. Therefore, the 1,776,245 grid is more suitable. The same calculation method is used to verify the grids of the other models. The meshes of a smooth channel, a square roughness element, sharp angle roughness element and triangular roughness element are 836,536, 1,776,245, 1,651,650 and 1,572,370 respectively.

3.4.2. Model validation

The gas flow fields in smooth channel and rectangular rough element channel were verified. Fig. 5 shows the mean velocities in the smooth channel with the X = 0.3 m cross section. The results of RSM simulation are in good agreement with those of Kim et al.

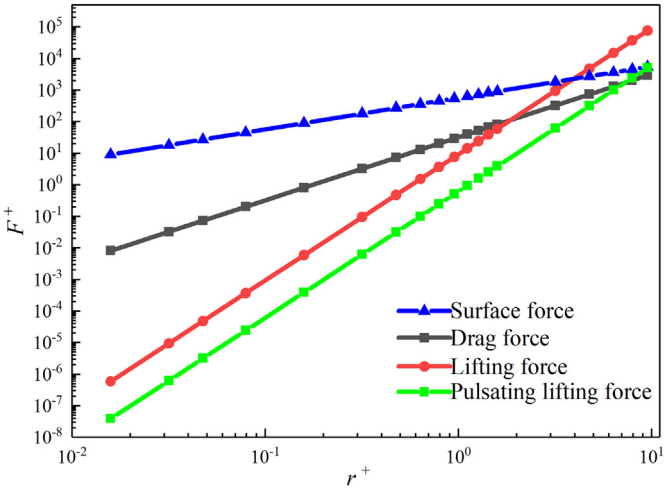

Fig. 3. The force of particles varies with dimensionless radius.

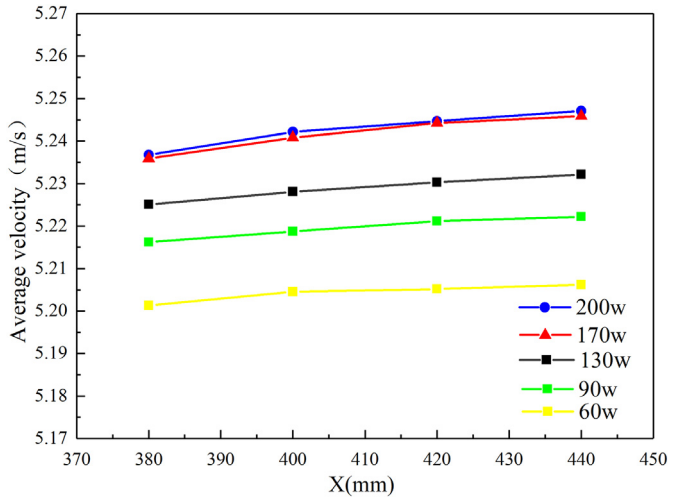

Fig. 4. Grid independence verification.

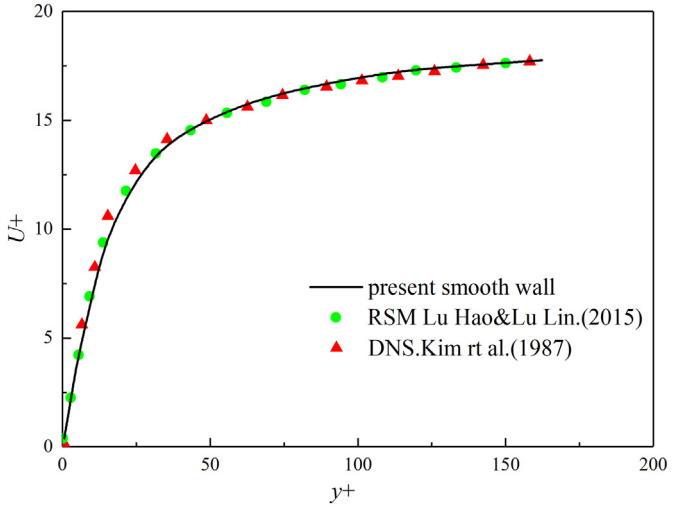

Fig. 5. Verification of flow velocity in smooth channel.

[31]. and Lu et al. [22]. The average relative errors were 3.25% and 1.7%, respectively. As shown in Fig. 6 and Table 3, for the eddy structure near the rough element in rough channel, the calculated eddy length is in good agreement with Casarsa and Arts [32] as well as Lecrivain et al. [13], which shows that the RSM model can simulate turbulent flow in a rough channel very well.

The average relative errors can be expressed as:

$$\eta_{ave} = \frac{1}{n}\sum_{i=1}^{n}\frac{|\nu_i - \hat{\nu}_i|}{\hat{\nu}_i} \tag{17}$$

To accurately simulate particle deposition in a rough channel, the particle deposition in a smooth channel is calculated. Fig. 7 shows the relationship between dimensionless relaxation time and dimensionless deposition velocity in a smooth channel. It can be seen that the results of this paper are in good agreement with those of Tian and Amadi [27], Montgomery and Core [33], Zhang and Chen [34], and Kvasnak et al. [35]. So CFD-DEM can accurately simulate the deposition characteristics of particles.

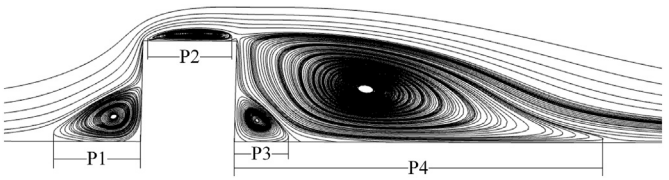

Fig. 6. Vortex structure near rough element.

3.5. Computation of particle deposition velocity and ratio

Particle deposition velocity V_d is usually introduced to represent the characteristics of particle deposition, and its expression is defined as [36],

$$V_d = -\frac{hU_0 \ln(1-N_{dep}/N_{in})}{L} \tag{16}$$

where h is the height of the computation area, L is the length of the computation area, U_0 is the average velocity, N_{dep} is the deposition number of particles on the surface, and N_{in} is the total number of particles entering the computation area.

Dimensionless particle deposition velocity and dimensionless relaxation time are usually used to express the particle deposition velocity. Among them, the dimensionless deposition rate is defined as:

$$V_d^{+} = V_d/u^{*} \tag{17}$$

The dimensionless relaxation time is defined as:

$$\tau_p^{+} = \frac{Sd_p u^{*2}}{18\nu^2} C_c \tag{18}$$

where S is gas-solid density ratio, and C_c is a Canningham coefficient, which is further defined as:

$$C_c = 1 + \frac{2\lambda}{d}\left[1.257 + 0.4e^{-(1.1d_p/2\lambda)}\right] \tag{19}$$

where the λ is the gas molecular mean free path.

4. Results and discussion

4.1. Air flow simulation

The first half of the rough channel has a smooth wall, and the second half has nine rough elements on the upper and lower walls. Because of

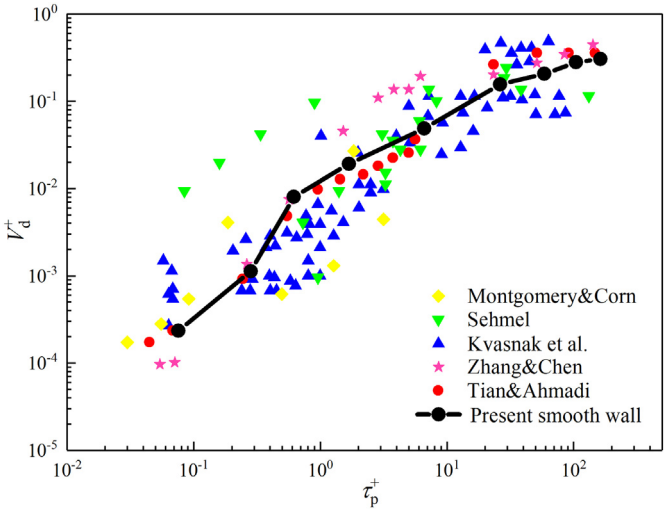

Fig. 7. Verification of particle deposition velocity in smooth tube.

the existence of rough elements, the wall boundary layer gradually thickens from the first rough structure until the fifth rough structure becomes stable. The flow field near the sixth and seventh rough element was selected for analysis, as shown in Fig. 8. Rough structure reduces the cross-section area of the channel, and the central velocity of the channel reaches 1.8 times that of the inlet velocity. At the same time, eddies of different sizes appear near the rough structures. The larger the angle between the windward side and the direction of airflow, the greater the fluctuation of airflow in the channel; the larger the angle between the leeward side and the direction of airflow, the longer the length of the vortex formed on the leeward side, thereby prolonging the residence time of particles in the channel.

4.2. Effect of rough structure shape on particle deposition velocity

Fig. 9 shows the velocity comparison of an infinite depositor in a smooth channel and rough channel (square rough structure). According to Wood [7], particle deposition can be divided into three regions $0.1<\tau_p^+<10$ (eddy diffusion collision zone), $\tau_p^+<0.1$ (turbulent diffusion zone), $\tau_p^+>10$ (inertial collision zone). The results show that with the particle diameter increases, the particle deposition rate gradually increases. It can be seen from the track diagram of the particle in Fig. 10 that the absorption capacity of small particles by vortex is stronger than that of large diameter particles. When $\tau_p^+>10$, the deposition rate of particles in a smooth channel is higher than that in rough channel. The main reason is that the larger the particle size, the larger the mass and inertia. Particle deposition is mainly influenced by its inertia and gravity. It is difficult to capture particles by eddies near rough elements. Because rough elements were arranged on the upper and lower surfaces of the rough flow channel, the flow velocity in the center region of the flow channel was increased, and some particles came out with the flow before deposition. When $0.1<\tau_p^+<1$, the particle deposition velocity in the rough channel is higher than that in the smooth channel.

Fig. 11 shows the particle deposition in a square rough element channel and a smooth channel at 1 μm For the convenience of observing the particle deposition location, the particles are displayed by points. It can be seen from the figure that the particle diameter is small and easy to be entrained by the eddies near the rough structure, which increases the probability of collision and rebound between the particles and the wall, resulting in the increase of particle deposition in the rough channel. Especially for particles

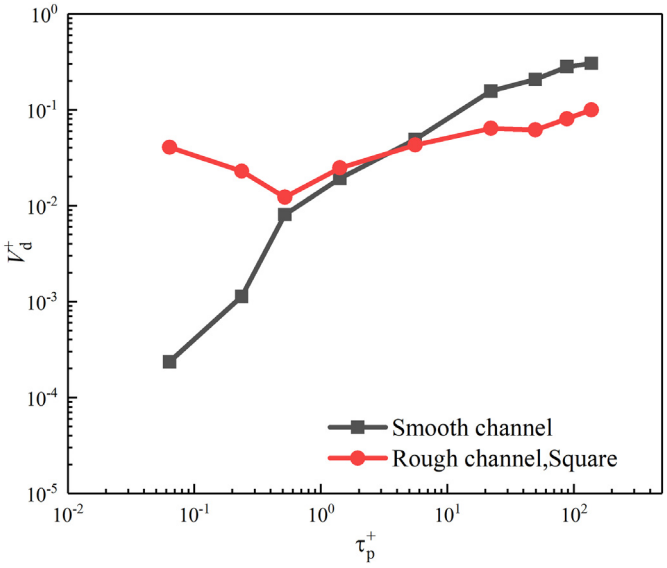

Fig. 9. Dimensionless deposition velocity in smooth channel and rough channels.

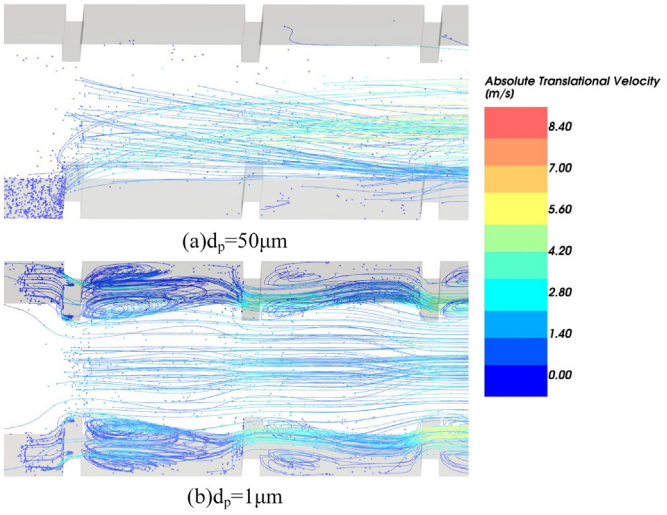

Fig. 10. Particle trajectory.

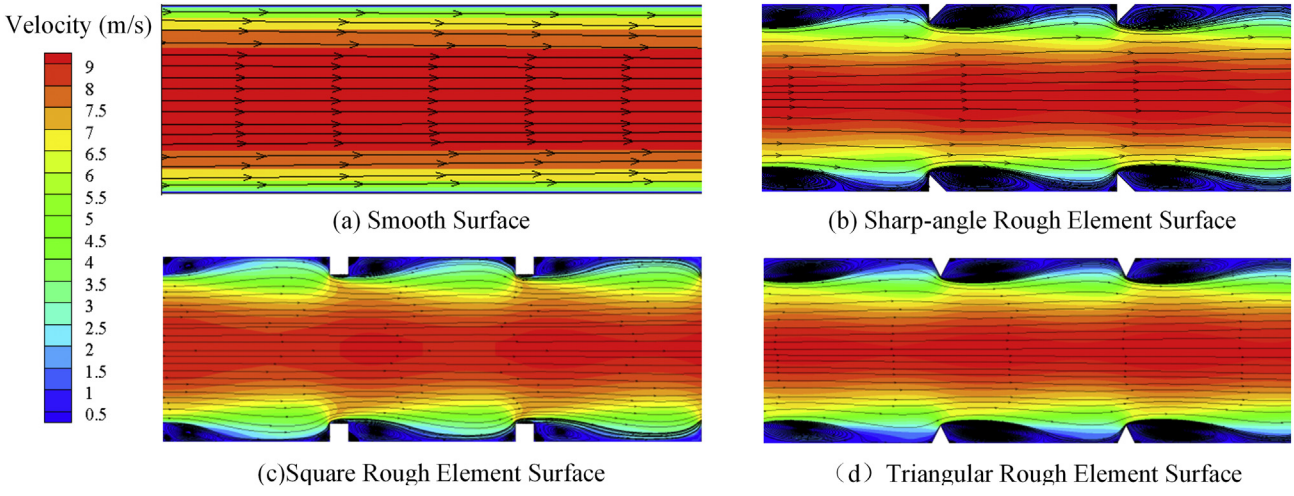

Fig. 8. Velocity distribution in smooth and rough channels.

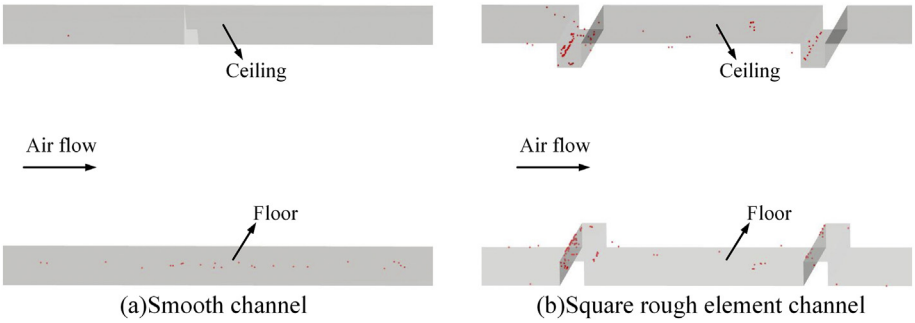

Fig. 11. Deposition of 1 μm particles in rough channel and smooth channel.

with $d_p < 10$ μm, the van der Waals adhesion force is 2–4 orders of magnitude greater then gravity. The increase of the van der Waals adhesion force leads to the increase of the deposition rate of small particles. At this time, particle deposition is mainly affected by eddies, inertia and adhesion forces near rough structures.

In order to analyze the effect of rough element shapes on particle deposition, In this paper, particle deposition in a rough channel with square, sharp angle and triangular structures, which were simulated in that order. The particle deposition mechanism includes inertial impact, turbulent deposition, interception, diffusion and so on. Inertial impact is one of the most important mechanisms in particle deposition.

Fig. 12 shows the effect of the rough element structure on the dimensionless deposition rate of particles. The particle deposition rate of a triangular rough element channel was obviously lower than that of the other two rough structures.

As shown in Fig. 13, the particles in sharp-angle and triangular rough channels after impact with the first rough element windward surface can be seen. After impact on the windward surface of the sharp-angle rough structure, some particles entered the channel with gas, and the other particles collided and deposited on the downward wall. The angle between the upwind surface of the triangular rough structure and the direction of gas flow was less than 90°, and the interception effect of the rough element on the incoming particles decreased. At this time, most particles enter the central region of the channel with the gas after collision with the upwind surface, which leads to a decrease of deposition, and the upwind surface plays a role in assisting particles to move towards the center of the channel. The interception effect was significantly enhanced with the increase of particle diameter.

For sharp-angle and square rough element channels, When $d_p > 5$ μm, the deposition rate of particles remains unchanged. This shows that the particle deposition velocity is independent of the shape of the rough element, but only related to the angle between the windward surface of the rough element and the horizontal direction. When $d_p < 5$ μm, the dimensionless deposition velocity of the forward sharp-angle rough element channel is higher than that of the square rough element channel. Because the particle size is small, it is easy to be entrained by turbulent eddies near rough elements. At the same time, the length of the eddy behind the leeward surface is longer, which prolongs the residence time of the particles near the eddy and leads to the increase of the deposition velocity of the particles.

4.3. Effect of surface energy on particle deposition velocity

Different substances in nature have different surface energies. The free energy of solid surface is the main factor causing the deposition of micro-particles on the wall. The adhesion of particles to the wall after collision depends on the material properties of the wall. Surface energy determines the adsorption properties of particles on the wall. In this paper, the deposition velocity of particles in a channel with a diameter of 10 μm and 50 μm and a surface energy of (0.01 J/m^2–0.1 J/m^2) is

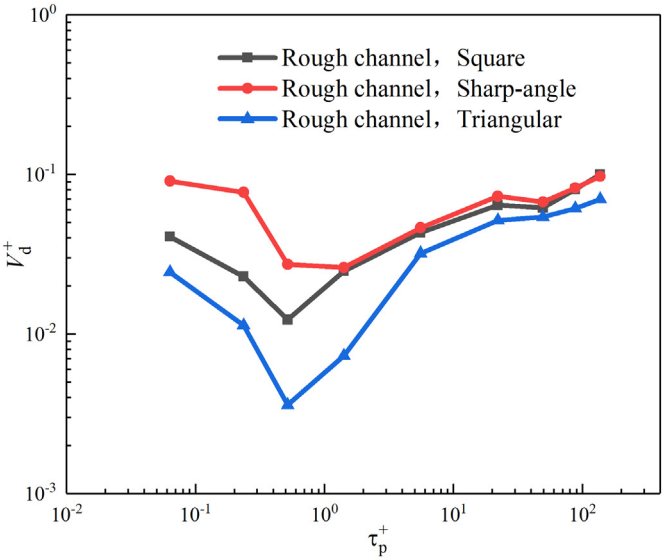

Fig. 12. Effect of rough element structure on dimensionless deposition velocity of particles.

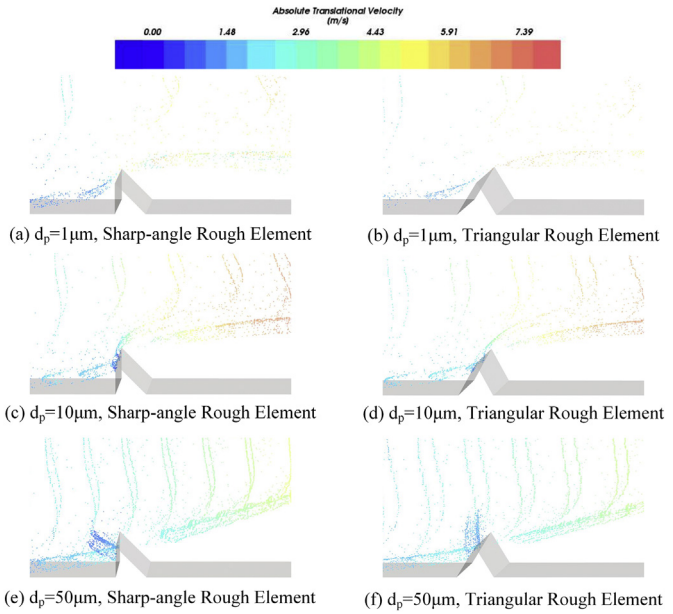

Fig. 13. Distribution of 1, 10, 50 μm particles in rough channel at different times.

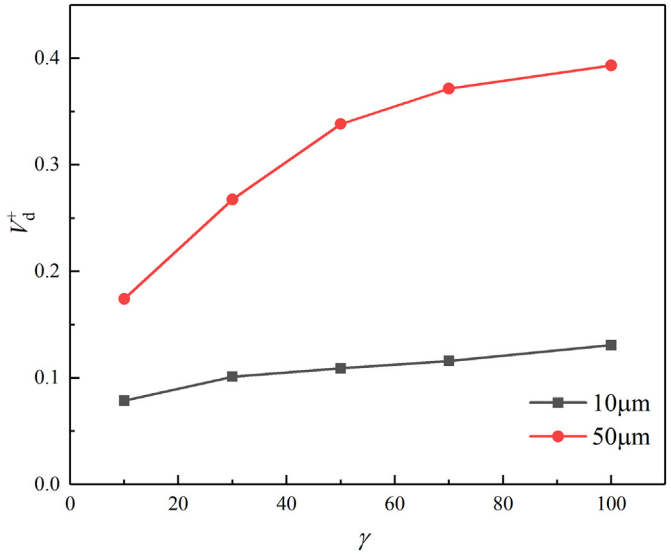

Fig. 14. Deposition velocities of different surface energy particles.

studied for a sharp-angle rough element channel with a bottom surface. As shown in Fig. 14 it can be found that the deposition rate of particles increases with the increase of surface energy. Moreover, the deposition rate of large particles increases faster than that of small particles. Therefore, particle deposition can be enhanced by using materials with higher surface energy.

5. Conclusion

In this paper, the CFD-DEM coupling method is used to study the wall-approaching characteristics of particles in different shapes of rough element channels. The conclusions are as follows:

1. Because of the existence of a rough structure on the wall, the eddy recirculation zone near the rough elements makes the deposition rate of $0.1<\tau_p^+<1$ particles in the rough channel increase greatly compared with that in the smooth channel, and the deposition rate of 1 μm particles increases 172 times. The medium particle $1<\tau_p^+<10$ increased little; For $\tau_p^+>10$, the deposition rate of the smooth channel is higher than that of the rough channel.
2. For different shapes of rough structure channels, the windward surface of a rough structure has a strong interception effect. The smaller the angle between the windward surface and airflow direction, the smaller the interception effect and the smaller the deposition rate of particles. With the increase of the angle between the leeward surface and airflow direction, the trapping effect of eddies on small particles is enhanced.
3. With the increase of wall surface energy, the deposition rate of particles increases with the same particle size. Therefore, increasing the surface energy of the wall can be used as an effective means to enhance the particles in the pipeline.

Acknowledgment

This study was funded by the National Natural Science Foundation of China (No. 51776032).

Nomenclature

C_c	Cunningham slip correction factor
d_p:	particle diameter
F^+	dimensionless forces
F_D	particle drag force
$F_{L,saffman}$	Saffman lift force
F_{po}	Van der Waals adhesion force
$F_{contact}$	Contact force
F_{Mag}	Magnus force
h	channel diameter
I	the particle rotation inertia
L:	the length of channel
M_F	fluid action moment
M_A	Van der Waals adhesion Moment and Particle Collision Moment
m_p	particle mass
N_{dep}:	particle deposition numbers to wall
N_{in}	incoming particle numbers
r_p^+	dimensionless radius
r_p:	particle radius
r_{eq}	contact radius
S	ratio of particle-to-fluid density
U_0	average velocity of air
u_{pi}	the particle translation velocity
u^*	frictional velocity of air
u_{px}	axial velocity of particles
V_d	particle deposition velocity
V_d^+	non-dimensional deposition velocity
y^+	dimensionless distance
y	the distance from the wall

Greek symbols

γ	surface energy
η_{ave}	average relative errors
λ	is the gas molecular mean free path
μ	dynamic viscosity of air
μ_f	Sliding friction coefficient between particles and wall
ν	kinetic viscosity of air
ρ	air density
τ_p^+	non-dimensional particle relaxation time
τ_w	shear stress on the wall
Ψ	Stokes drag force correction factor
Ω	the particle rotation velocity

References

[1] M. Krafczyk, J. Linxweiler, M. Stiebler, Inner-Urban Air Flow Simulations to Predict Fine Dust Pollution of Anthropogenic Sources Using LES-LBM on Multiple GPGPUs.
[2] L. Megido, B. Suarez-Pena, L. Negral, L. Castrillon, Y. Fernandez-Nava, Suburban air quality: human health hazard assessment of potentially toxic elements in PM10, Chemosphere 177 (2017) 284–291.
[3] A. Li, G. Ahmadi, R.G. Bayer, M.A. Gaynes, Aerosol particle deposition in an obstructed turbulent duct flow, J. Aerosol Sci. 25 (1994) 91–112.
[4] J.S. Yong, K. Sang Soo, Effect of obstructions on the particle collection efficiency in a two-stage electrostatic precipitator, J. Aerosol Sci. 27 (1996) 61–74.
[5] P.G. Papavergos, A.B. Hedley, Particle Deposition Behaviour in Fully Developed Turbulent Flows, Multiphase Transport: Fundamentals, Reactor Safety, Applications, 1980.
[6] M.W. Reeks, G. Skyrme, The dependence of particle deposition velocity on particle inertia in turbulent pipe flow, J. Aerosol Sci. 7 (1976) 485–495.
[7] N.B. Wood, A simple method for the calculation of turbulent deposition to smooth and rough surfaces, J. Aerosol Sci. 12 (1981) 0–290.
[8] M.R. Sippola, W.W. Nazaroff, Experiments measuring particle deposition from fully developed turbulent flow in ventilation ducts, Aerosol Sci. Technol. 38 (2004) 914–925.
[9] B.Y.H. Liu, J.K. Agarwal, Experimental observation of aerosol deposition in turbulent flow, J. Aerosol Sci. 5 (1974)145,IN141,149-148,IN142,155.
[10] M. Sommerfeld, J. Kussin, Wall roughness effects on pneumatic conveying of spherical particles in a narrow horizontal channel, Powder Technol. 142 (2004) 180–192.
[11] A. Deshmukh, V. Vasava, A. Patankar, M. Bose, Particle velocity distribution in a flow of gas-solid mixture through a horizontal channel, Powder Technol. 298 (2016) 119–129.
[12] T. Barth, M. Reiche, M. Banowski, M. Oppermann, U. Hampel, Experimental investigation of multilayer particle deposition and resuspension between periodic steps in turbulent flows, J. Aerosol Sci. 64 (2013) 111–124.
[13] G. Lecrivain, L. Barry, U. Hampel, Three-dimensional simulation of multilayer particle deposition in an obstructed channel flow, Powder Technol. 258 (2014) 134–143.

[14] G. Lecrivain, D.-M. Sevan, B. Thomas, U. Hampel, Numerical simulation of multilayer deposition in an obstructed channel flow, Adv. Powder Technol. 25 (2014) 310–320.
[15] B. Zhao, J. Wu, Modeling particle deposition onto rough walls in ventilation duct, Atmos. Environ. 40 (2006) 6918–6927.
[16] B. Milici, Modification of particle laden near-wall turbulence in a vertical channel bounded by rough walls, Int. J. Multiph. Flow 103 (2018) 151–168.
[17] S. Matsusaka, W. Theerachaisupakij, H. Yoshida, H. Masuda, Deposition layers formed by a turbulent aerosol flow of micron and sub-micron particles, Powder Technol. 118 (2001) 130–135.
[18] G.L. Iacono, P.G. Tucker, A.M. Reynolds, Predictions for particle deposition from LES of ribbed channel flow, Int. J. Heat Fluid Flow 26 (2005) 558–568.
[19] A.C.K. Lai, M.A. Byrne, A.J.H. Goddard, Measured deposition of aerosol particles on a two-dimensional ribbed surface in a turbulent duct flow, J. Aerosol Sci. 30 (1999) 1201–1214.
[20] A.C.K. Lai, M.A. Byrne, A.J.H. Goddard, Aerosol deposition in turbulent channel flow on a regular array of three-dimensional roughness elements, J. Aerosol Sci. 32 (2001) 121–137.
[21] H. Lu, L. Lu, Effects of rib spacing and height on particle deposition in ribbed duct air flows, Build. Environ. 92 (2015) 317–327.
[22] H. Lu, L. Lu, CFD investigation on particle deposition in aligned and staggered ribbed duct air flows, Appl. Therm. Eng. 93 (2016) 697–706.
[23] C.D. Dritselis, On the enhancement of particle deposition in turbulent channel airflow by a ribbed wall, Adv. Powder Technol. 28 (2017) 922–931.
[24] M. Afkhami, A. Hassanpour, M. Fairweather, Effect of Reynolds number on particle interaction and agglomeration in turbulent channel flow, Powder Technol. 343 (2019) 908–920.
[25] H. Zhang, F.X. Trias, A. Gorobets, A. Oliva, D. Yang, Y. Tan, Y. Sheng, Effect of collisions on the particle behavior in a turbulent square duct flow, Powder Technol. 269 (2015) 320–336.
[26] J.S. Marshall, Q. Yao, S.Q. Li, A. Ratner, Molecular dynamics simulation of particle deposition and agglomeration in two-phase dilute flow, J. Eng. Thermophys. 28 (2007) 1035–1038.
[27] L. Tian, G. Ahmadi, Particle deposition in turbulent duct flows—comparisons of different model predictions, J. Aerosol Sci. 38 (2007) 377–397.
[28] J.K. Eaton, J.R. Fessler, Preferential concentration of particles by turbulence, Phys. Fluids A Fluid Dyn. 3 (1991) 169–209.
[29] B. Wang, H.Q. Zhang, X.L. Wang, Large eddy simulation of particle response to turbulence along its trajectory in a backward-facing step turbulent flow, Int. J. Heat Mass Transf. 49 (2006) 415–420.
[30] M.E. O'Neill, A sphere in contact with a plane wall in a slow linear shear flow, Chem. Eng. Sci. 23 (1968) 1293–1298.
[31] J. Kim, P. Moin, R. Moser, The Turbulence Statistics in Fully Developed Channel Flow at Low Reynolds Number, 1987.
[32] A. Armellini, L. Casarsa, C. Mucignat, Experimental assessment of the aero-thermal performance of rib roughened trailing edge cooling channels for gas turbine blades, Appl. Therm. Eng. 58 (2013) 455–464.
[33] T.L. Montgomery, M. Corn, Aerosol deposition in a pipe with turbulent airflow, J. Aerosol Sci. 1 (1970) 185–213.
[34] Z. Zhang, Q. Chen, Prediction of particle deposition onto indoor surfaces by CFD with a modified Lagrangian method, Atmos. Environ. 43 (2009) 319–328.
[35] W. Kvasnak, G. Ahmadi, R. Bayer, M. Gaynes, Experimental investigation of dust particle deposition in a turbulent channel flow, J. Aerosol Sci. 24 (1993) 795–815.
[36] H. Liu, Z. Li, Prediction of particle deposition characteristic in 90° square bend: square bend particle deposition characteristic, Appl. Therm. Eng. 31 (2011) 3402–3409.